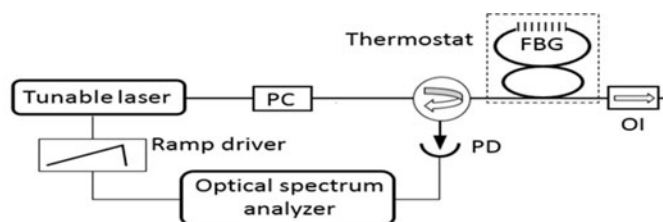


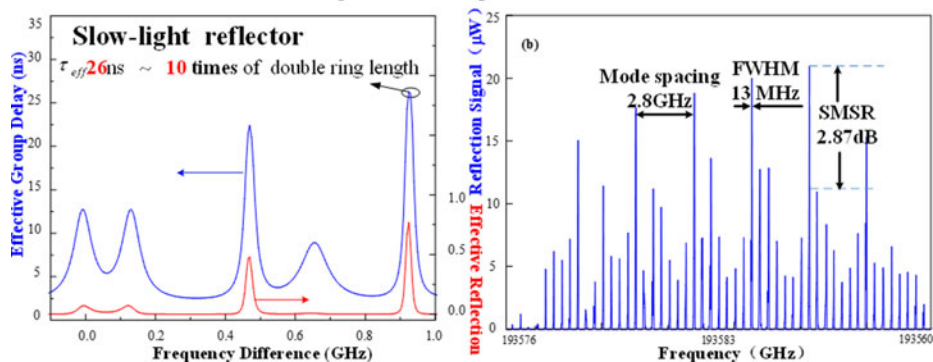
Slow-Light Effect and Mode Selection of Double Fiber Ring With a Fiber Bragg Grating

Volume 10, Number 1, February 2018

Xiaoqiong Qin
Zujie Fang
Kang Ying
Zhidan Ding
Di Wang
Fang Wei
Fei Yang
Qing Ye
Ronghui Qu
Haiwen Cai



Measurement setup of double ring resonator's characteristics



Mode hopping suppression of narrow linewidth lasers, Enhancing resolution of sensors

DOI: 10.1109/JPHOT.2017.2782663

1943-0655 © 2017 IEEE

Slow-Light Effect and Mode Selection of Double Fiber Ring With a Fiber Bragg Grating

Xiaoqiong Qin^{1,2}, Zujie Fang,¹ Kang Ying¹, Zhidan Ding,^{1,2}
Di Wang,^{1,2} Fang Wei,¹ Fei Yang,¹ Qing Ye,¹ Ronghui Qu,¹
and Haiwen Cai¹

¹Shanghai Key Laboratory of All Solid-State Laser and Applied Techniques, Shanghai Institute of Optics and Fine Mechanics, Chinese Academy of Sciences, Shanghai 201800, China

²University of Chinese Academy of Sciences, Beijing 100049, China

DOI:10.1109/JPHOT.2017.2782663

1943-0655 © 2017 IEEE. Translations and content mining are permitted for academic research only.

Personal use is also permitted, but republication/redistribution requires IEEE permission.

See http://www.ieee.org/publications_standards/publications/rights/index.html for more information.

Manuscript received October 8, 2017; revised December 1, 2017; accepted December 8, 2017. Date of publication December 12, 2017; date of current version January 8, 2018. This work was supported in part by the National Natural Science Foundation of China under Grants 61775225, 61405218, 61535014, and 61475165, in part by the National Basic Research Program of China under Grant 2017YFB0405500, in part by the Shanghai City Foundation for Leaders of Disciplines in Technology under Grant 15XD1524500, and in part by the Scientific innovation fund of Chinese Academy of Sciences under Grant CXJJ-17S010. Corresponding authors: K. Ying and H. Cai (e-mail: yingk0917@siom.ac.cn; hwcai@siom.ac.cn).

Abstract: A novel slow-light reflector composed of a double-ring resonator with a uniform fiber Bragg grating (FBG) incorporated is proposed in this paper, which can be used as a mirror of narrow-linewidth fiber laser, based on its enlarged group delay, and as a high-sensitivity sensor. Its characteristics are investigated theoretically and experimentally in this paper. Compared with the single fiber ring the amplitude of resonance is modulated, the effective mode spacing is expanded greatly, due to the Vernier effect, giving much better mode selectivity. Mode hopping is believed to be suppressed effectively in applications of narrow-linewidth lasers, and resolution will be enhanced in sensor applications.

Index Terms: Fiber ring, fiber Bragg grating, fiber laser, slow-light effect.

1. Introduction

Fiber ring is a compact all-fiber resonator [1]–[3] with narrow linewidth resonances, when the split ratio of coupler is low enough, used widely as phase modulators [4], [5], [20], ring cavity Brillouin lasers [6], [7], [21], sensors [8], [9], etc. It is an all-pass filter if losses of fiber and coupler can be neglected. When a fiber Bragg grating (FBG) is inserted in the ring, narrow linewidth and high reflections occur at the resonances. Such a reflector is used as a cavity mirror of fiber laser with the linewidth is narrowed down to 150 Hz, and the intrinsic Lorentzian linewidth down to 10 Hz. Compared with the F-P type laser, a linewidth reduction of more than 27 was obtained [10]. The characteristics of such a composite ring are investigated in [11]. It is indicated that the multiple CW and CCW circulating propagations in the ring lead to a greatly enlarged group delay, i.e., resulting in a slow-light effect [12]–[16], and the optimization of parameters is discussed, especially the split ratio of fiber coupler and the reflectivity of FBG. Such an effect is also attractive for fiber sensor applications [9], [22] and for photonic devices [17].

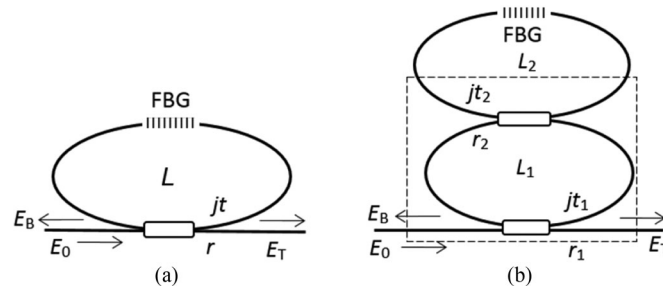


Fig. 1. Single ring (a) and double ring (b) with FBG inserted.

The free spectral range (FSR) of fiber ring is quite narrow since the fiber has to be long enough to build a ring with the fiber coupler. It is thus not easy to keep the laser in a single longitudinal mode; and not easy to avoid mode hopping since the longer fiber is susceptible to environmental vibrations and temperature changes. For sensor applications, a narrow and stable filter is needed to select one resonance.

To enlarge the mode spacing for suppression of mode hopping, a novel structure with a double ring is proposed and demonstrated, in which the resonances will be modulated by the so-called Vernier effect, and the effective mode spacing will be enlarged. The characteristics of double ring with FBG are analyzed theoretically and verified experimentally with different structure parameters in this paper.

2. Principle and Simulations

The slow-light reflector proposed in [10], [11] is shown in Fig. 1(a). It is known that the fiber ring is an all-pass filter with phase shift dependent on the wavelength. When an FBG is inserted in the ring, propagation in CCW way is generated, then the filter behaves as a beam splitter with resonant reflection. Its transfer function is deduced as

$$r_{eff} = \frac{E_B}{E_0} = \frac{-jt^2 r_g e^{j\beta L_2}}{1 - 2t_g r e^{j\beta L_2} + r^2 e^{j2\beta L_2}} \quad (1)$$

where t_g and r_g are the field transmission and reflection of FBG. In case the split ratio of the fiber coupler $\kappa = t^2$ is low enough, a very low reflectivity FBG with $R_g = |r_g|^2 \ll 1$ will show high reflection at resonances, expressed approximately as $R_{eff}^{[res]} \approx \kappa^2 R_g / (1 - \sqrt{1 - \kappa})^4 \approx 16R_g / \kappa^2$. More important, a greatly extended photon's lifetime $\tau_d^{[res]} \approx 4\tau\sqrt{1 - \kappa}/\kappa$ is obtained at the resonances. It is therefore suitable to be used as a cavity mirror of narrow linewidth fiber lasers. The slow-light effect was verified experimentally in [10], [11]. And a linewidth reduction of more than 27, compared with the F-P type laser, was obtained.

The fiber ring with FBG has attractive merits, especially the remarkable slow-effect and the low cost. When it is used as a cavity mirror of fiber laser, coincidence of the ring resonance, FBG peak, and laser's longitudinal modes is one of the necessary conditions for the fiber laser working stably. However, the FSR of $\lambda_{FSR} = \lambda^2 / (nL)$, is very narrow, due to the long fiber length. In [10] the fiber length was ~ 50 cm, and the spacing is about 400 MHz. Since the fiber index is sensitive to temperature changes and strains, the resonance frequencies may shift with the environmental conditions. The resonance frequencies vary with index fluctuations as

$$\delta\lambda_{res} = \frac{\lambda_{res}}{nL} \int_0^L \delta n(z, t) dz \quad (2a)$$

$$\delta\lambda_{res} / \lambda_{FSR} = \lambda_{res}^{-1} \int_0^L \delta n(z, t) dz \quad (2b)$$

It is shown that compared with FSR the fluctuation of resonance peak is a serious impact on the stability of lasing wavelength.

To overcome this shortcoming, we propose a new structure of double ring with FBG incorporated as shown in Fig. 1(b), where L_1 and L_2 are the lengths of two rings respectively, $t_{1,2}$ and $r_{1,2}$ are the optical field split ratios of two fiber couplers, respectively, with relations to power split ratios as $t_{1,2}^2 : r_{1,2}^2 = \kappa_{1,2} : (1 - \kappa_{1,2})$, and the phase shift of $\pi/2$ between two ports of the coupler is marked by the imaginary unit j . The effect of double ring cavity is the modulation of resonance amplitudes, due to Vernier effect, which is used often in selection of laser's longitudinal mode, such as in superstructure DBR lasers [18]. Such a modulation will effectively enhance the side mode suppression ratio (SMSR) of the resonances.

The formulas for a single ring with FBG incorporated given in [10] and [11] are referred here, but with a composite fiber coupler, as shown by the dashed line square in the Fig. 1(b), instead of a conventional broadband fiber coupler. The effective optical field split ratios of such a composite coupler are now complexes with modulus and phases deduced as

$$|r_c|^2 = \frac{r_1^2 + r_2^2 - 2r_1r_2 \cos \beta L_1}{1 + r_1^2 r_2^2 - 2r_1r_2 \cos \beta L_1}$$

$$\tan \varphi_r = \frac{-r_2(1 - r_1^2) \sin \beta L_1}{r_1(1 + r_2^2) - r_2(1 + r_1^2) \cos \beta L_1} \quad (3)$$

$$|t_c|^2 = \frac{t_1^2 t_2^2}{1 + r_1^2 r_2^2 - 2r_1r_2 \cos \beta L_1}$$

$$\tan \varphi_r = \frac{r_1 r_2 - \cos \beta L_1}{\sin \beta L_1} \quad (4)$$

The power split ratio of composite coupler is given by $\kappa_c = |t_c|^2$, which oscillates with period dependent on L_1 between $\kappa_{\max} = \kappa_1 \kappa_2 / (1 - r_1 r_2)^2$ and $\kappa_{\min} = \kappa_1 \kappa_2 / (1 + r_1 r_2)^2$.

By replacing the parameters of a plain fiber coupler by (3) and (4) in formula (1), the effective field reflectance and power reflectance are then obtained as

$$\frac{E_B}{E_0} = \frac{-j|t_c|^2 r_g e^{j(\beta L_2 + 2\varphi_r)}}{1 - 2t_g |r_c| e^{j(\beta L_2 + \varphi_r)} + |r_c|^2 e^{j2(\beta L_2 + \varphi_r)}} \quad (5)$$

$$\frac{I_B}{I_0} = \frac{|t_c|^4 r_g^2}{1 + 4t_g^2 |r_c|^2 + |r_c|^4 - 4t_g |r_c| (1 + |r_c|^2) \cos(\beta L_2 + \varphi_r) + 2|r_c|^2 \cos(2\beta L_2 + 2\varphi_r)}$$

$$\approx \frac{|t_c|^4 r_g^2}{[1 + |r_c|^2 - 2|r_c| \cos(\beta L_2 + \varphi_r)]^2} \quad (6)$$

where t_c , r_c and φ_r are sinusoidal functions of βL_1 , the resonances are now not with equal amplitudes, but modulated by a function determined by the two fiber lengths of L_1 and L_2 , and by the split ratios of two fiber couplers.

In formulas (5) and (6) the spectra of FBG reflection r_g and transmission t_g play important roles. A narrow linewidth FBG will help mode selectivity. The spectra of FBG field reflectance and transmittance are expressed for a uniform grating as [8]

$$r_g = \frac{-j\kappa_g \sinh \sigma L}{\sigma \cosh \sigma L - j\delta \sinh \sigma L} \quad (7)$$

$$t_g = \frac{\sigma e^{j\beta_B L}}{\sigma \cosh \sigma L - j\delta \sinh \sigma L} \quad (8)$$

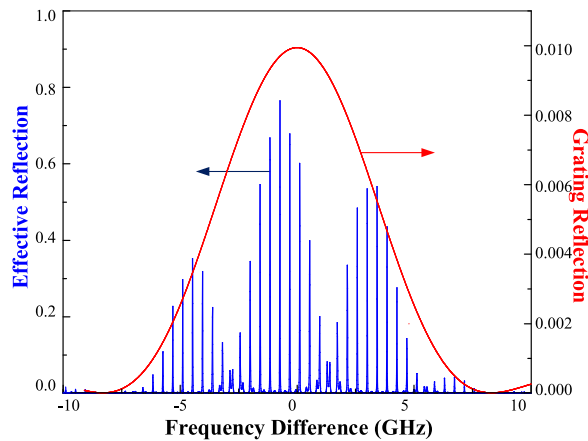


Fig. 2. Reflection spectra of FBG and double ring with FBG ($r_1 = 0.6$, $r_2 = 0.5$, $L_1 = 36$ cm, $L_2 = 40$ cm).

where $\delta = \beta - \beta_B$, $\sigma = \sqrt{\kappa_g^2 - \delta^2}$ with Bragg wave vector β_B , grating coupling coefficient κ_g , and the grating length L . The typical grating length is in the order of 10 mm, and linewidth in the order of 0.1 nm, which is usually much larger than the mode spacing of fiber ring.

The detailed analytical formulas for different parameters of r_1 , L_1 , r_2 , L_2 and r_g are quite tedious and lengthy, the digital calculations on the characteristics are surely necessary. The simulation results are given as follows.

2.1 Basic Characteristics of Double Ring With FBG Inserted

A typical spectrum of effective reflection of the double ring with FBG is shown in Fig. 2, where the parameters of simulation are taken as follows: split ratios of $r_1 = 0.6$, and $r_2 = 0.5$ ($\kappa_1 = 0.64$, $\kappa_2 = 0.75$), fiber lengths of $L_1 = 36$ cm and $L_2 = 40$ cm; FBG's peak reflectivity $R_g = 0.01$, with grating length $L = 1$ cm. The composite split ratio oscillates in the range between 0.3 and nearly 1.0. The central wavelength is set at 1550 nm, corresponding to optical frequency of 193.4 THz, which is taken as the middle point of abscissa of Fig. 2.

It is shown that the resonance amplitudes are modulated by the Vernier effect, the spacing between two envelope maxima is about 9 FSR. The reflection of FBG is greatly magnified by the double ring, the maximum reflection is almost 80 times of FBG's reflection.

2.2 Optimization of Side Mode Suppression Ratio

Higher modulation depth is beneficial for higher side mode suppression ratio (SMSR). Simulations indicate that it is dependent on the modulation depth and period of effective split ratio. The modulation period depends on the difference of ring's lengths, which is roughly estimated as $\Delta\lambda_{FSR} \propto L_1 L_2 / (L_2 - L_1)$, as discussed in [17]. A narrower modulation period results in a shaper roll-off at resonances, giving a larger SMSR.

Fig. 3(a) gives an example of simulation result with $r_1 = 0.6$, $r_2 = 0.5$, $L_1 = 36$ cm, $L_2 = 48$ cm. Although the spacing between envelope maxima is decreased compared with Fig. 2, a higher SMSR of 1.6 (~ 2.2 dB) between the main mode and the neighboring modes is obtained, much higher (~ 0.3 dB) than in Fig. 2. From the view of longitudinal mode stability of a fiber laser, characteristics of Fig. 3 is preferable.

Fig. 3(b) is the middle part of Fig. 3(a) with enlarged abscissa, the spectrum of effective split ratio of composite coupler is also depicted to show its modulation effect. From formula (3) the effective split ratio $|r_c|^2$ oscillates spectrally between $(r_1 + r_2)^2 / (1 + r_1 r_2)^2$ and $(r_1 - r_2)^2 / (1 - r_1 r_2)^2$, showing that a higher oscillation amplitude is obtained for a smaller difference of $(r_1 - r_2)$. It is seen

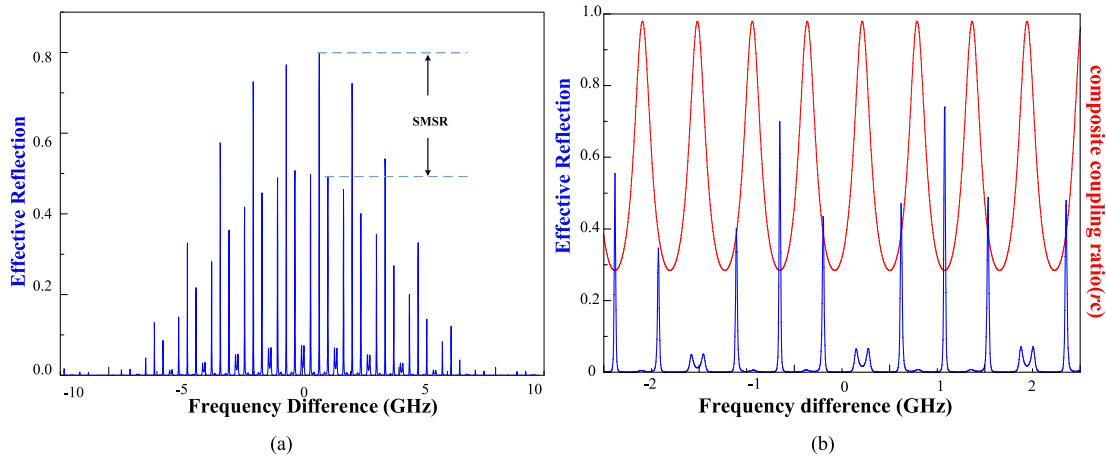


Fig. 3. (a) Effective reflection of double ring with FBG, for $r_1 = 0.6$, $r_2 = 0.5$, $L_1 = 36$ cm, $L_2 = 48$ cm; (b) Part of spectrum of (a), with the effective split ratio of composite coupler.

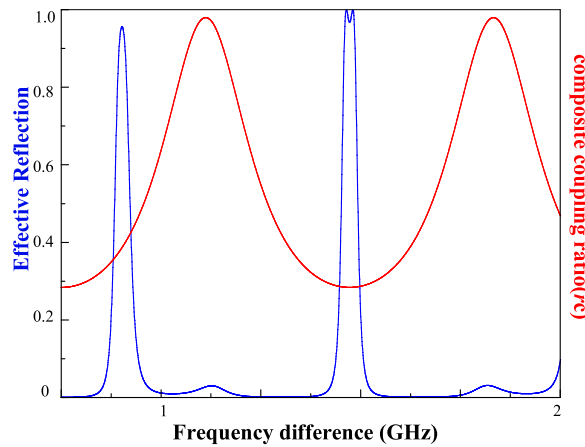


Fig. 4. Reflection spectrum of double ring with FBG of $R_g = 0.4$, showing a double peak resonance.

that the resonance amplitudes are modulated since its period is not equal to the period of split ratio oscillation, as shown in formula (6), and higher resonances appear at positions with lower split ratio, while lower resonances appear at positions with higher one. It is because the lower ratio leads to more circles of optical propagation in the ring, the same as the case of single ring.

As analyzed in [11] for a single ring with FBG, the reflectivity of FBG and the split ratio of fiber coupler should be low enough for a stronger slow-light effect, however a limitation exists, beyond which the effective reflection tends to beyond unity, and the total reflections occur off the resonant peaks, i.e., double peak resonances will appear. It is surely not good for a single longitudinal mode laser. The condition of single peak resonance is deduced in [11], expressed as

$$R_g < \kappa^2 / (2 - \kappa)^2 \quad (9)$$

The double peak resonances may also occur in the double ring. Fig. 4 shows an example in the case of $R_g = 0.04$ with other parameters same as Fig. 3(a). It is worthy of noticing that condition (9) can be loosened in a certain degree for the case of double ring, because the system has more adjustable parameters to find conditions of preventing the double peak resonance.

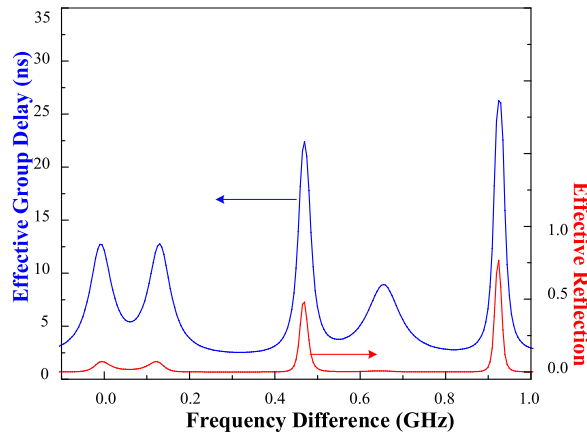


Fig. 5. Effective group delay of double ring with FBG.

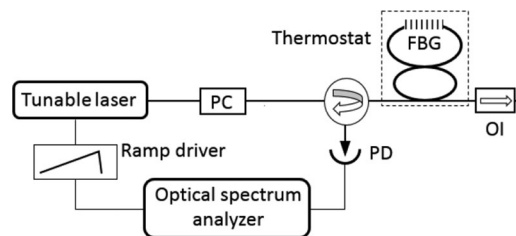


Fig. 6. Measurement setup of double ring resonator's characteristics, PC: polarization controller, OI: optical isolator.

2.3 Linewidth and Group Delay at Resonances

The linewidth at resonances is given in the simulations. The typical linewidth read from the data of Fig. 3 is 24 MHz, correspondingly with finesse of 19, which is similar to those of the single ring with FBG given in [11]. If the spacing between two envelope maxima is taken as FSR, the finesse is increased to 76 effectively. Different fiber lengths and split ratios of the couplers will give different results, qualitatively the behaviors are similar to the case of single ring, as analyzed in [11].

The effective phase shift of the double ring with FBG can be deduced from formula (5), expressed as

$$\phi_{eff} = \arctan \frac{2t_g |r_c| \sin(\beta L_2 + \varphi_r) - |r_c|^2 \sin[2(\beta L_2 + \varphi_r)]}{1 - 2t_g |r_c| \cos(\beta L_2 + \varphi_r) + |r_c|^2 \cos[2(\beta L_2 + \varphi_r)]} \quad (10)$$

The group delay is then calculated by $\tau_{eff} = \partial \phi_{eff} / \partial \omega$. Fig. 5 shows a simulated result as an example, where the blue line represents the effective group delay, the red line is for the effective reflectance of composite coupler. The parameters are the same as those used for Fig. 3. It is seen that greatly extended group delays are obtained at the resonances. The group delay of resonance at $\Delta f \sim 0.93$ GHz is calculated as 26 ns, corresponding to fiber length of 5.2 m, about 10 times of the ring length.

3. Experimental Results

To verify the above analysis characteristics of the double ring resonator are investigated in detail with a measurement system shown in Fig. 6, where a tunable laser is provided by the optical spectrum analyzer (APEX Technologies AP2041B) with linewidth of 500 kHz. The reflection spectra are displayed by the optical spectrum analyzer (APEX, AP2041B). The experimental results are as follows.

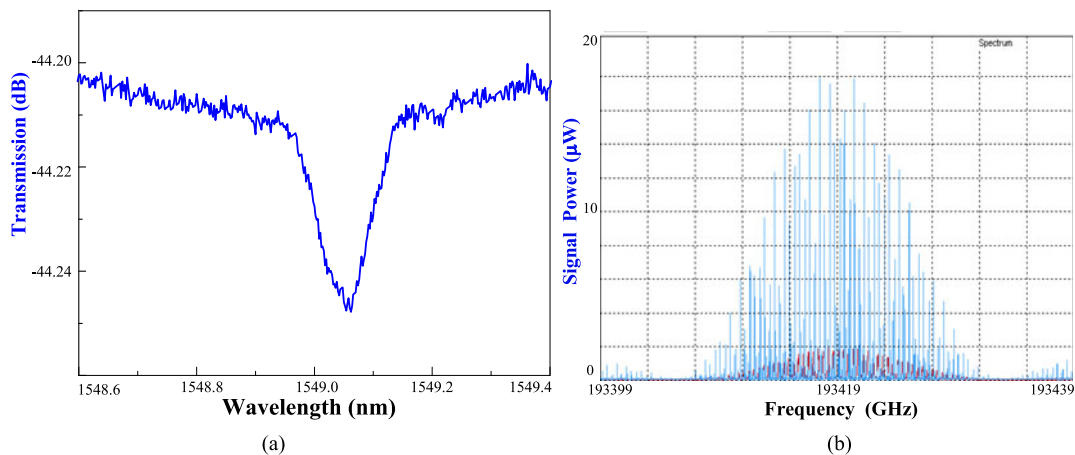


Fig. 7. (a) FBG transmission spectrum measured solitarily; (b) Reflection spectra of a single ring (red line) and a double ring (blue line) with the FBG inserted.

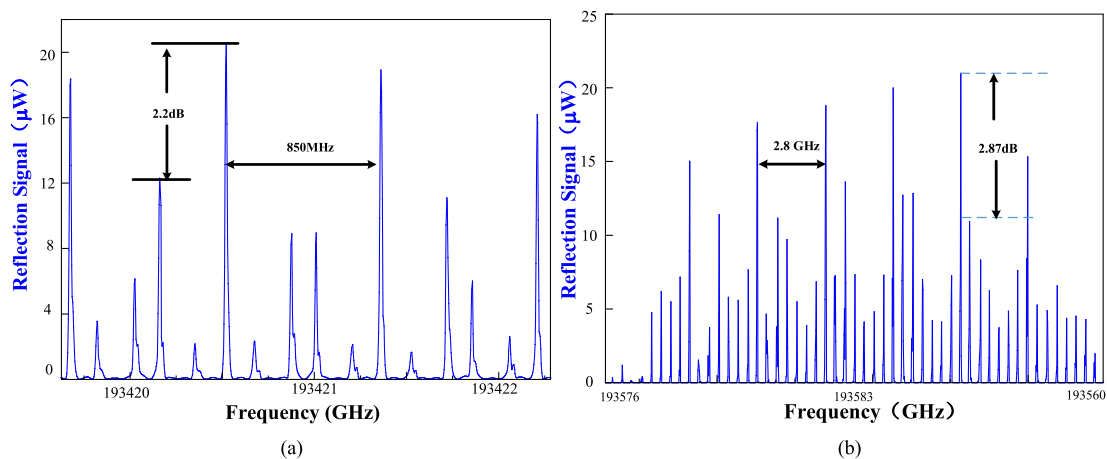


Fig. 8. (a) Detailed spectrum of Fig. 7(b); (b) Reflection spectrum of double ring with $L_1 = 60$ cm, $L_2 = 50$ cm, $\kappa_1 = 0.2$, $\kappa_2 = 0.15$.

3.1 Enhancement of FBG Reflectivity

The FBG reflectivity is enhanced greatly due to the double ring resonance. The FBG transmission spectrum is shown in Fig. 7(a), which is measured by using an ASE source and the optical spectrum analyzer. The dip is 0.04 dB, corresponding to $R_g = 0.9\%$, the Bragg wavelength is $\lambda = 1549.13$ nm. Fig. 7(b) gives the reflection spectra when inserted in a double ring with $\kappa_1 = 0.4$, $\kappa_2 = 0.9$, $L_1 = 69$ cm and $L_2 = 49.5$ cm by the blue line, and inserted in a single ring with $\kappa = 0.9$ by the red line. It is seen that the reflection amplitude of the former is nearly 10 times larger than that of the latter. Even the much lower side lobe of FBG reflection can be displayed by the double ring resonator.

3.2 Enhancement of FSR and SMSR

The enhancement of FSR and SMSR of the resonances by the double ring are verified experimentally. Fig. 8(a) shows the detailed spectrum of a part of Fig. 7(b). It is seen that the spacing between the main mode and the second highest mode is 850 MHz, about 5 FSR, the mode amplitude ratio between the main mode and the second side mode reaches 2.2 dB, which is thought pretty enough for mode-hopping suppression if it is used in fiber laser.

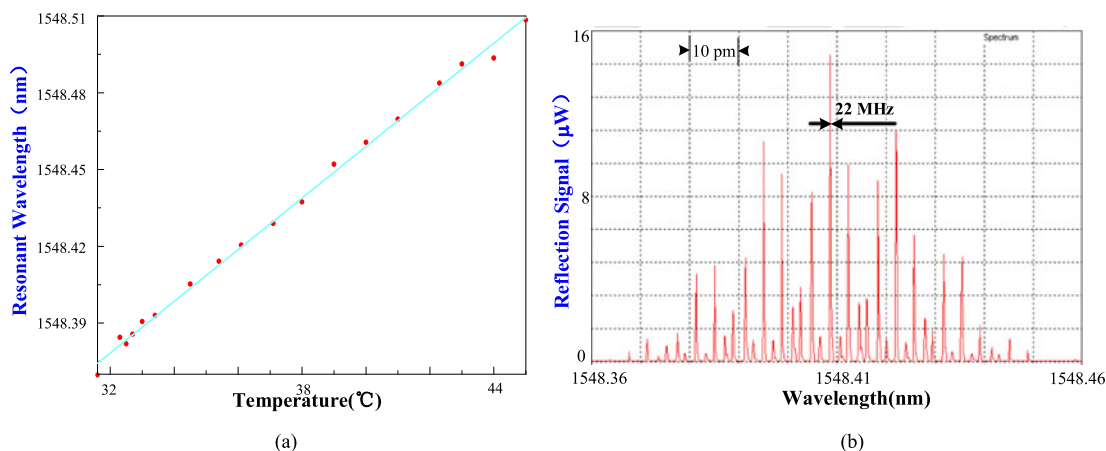


Fig. 9. (a) Resonant wavelength variation with temperature of the double ring with FBG; (b) Reflection spectrum at 35 °C.

The FSR and SMSR can be further optimized by changing the fiber lengths and the split ratios of couplers. Fig. 8(b) shows the measured spectrum with $L_1 = 60$ cm, $L_2 = 50$ cm, $\kappa_1 = 0.2$, $\kappa_2 = 0.15$, and the same FBG as used for Fig. 7(b). It is seen that the spacing between envelop maxima reaches 2.8 GHz, about 7 FSR. A typical SMSR between the main and neighboring resonances is 1.94, i.e., ~ 2.87 dB.

Compared with the single ring the linewidth of resonances will be narrowed further by stronger oscillations in the double ring. The FWHM linewidth of main mode is read 12.6 MHz in the measured spectrum of Fig. 7(b), one order narrower than that of the same FBG inserted in a single ring, which is measured 133 MHz.

3.3 Temperature Dependence of Double Ring's Resonance

Apart from the applications in narrow linewidth lasers, the fiber ring incorporated with FBG is also useful in sensor applications and photonic devices [9], [17]. Linewidths of ring resonances will be much narrower than that of FBG; therefore sensors will have a much high resolution. In both of the applications, the thermal stability or the thermal sensitivity is concerned mostly in practice. The temperature dependence of double ring with FBG is measured experimentally. The double ring is put in a water tank as a thermostat, whose temperature is adjusted in step of ~ 1 °C; during the temperature change, shift of the resonant peak to be measured is monitored carefully.

Fig. 9(a) gives the measured result of resonant wavelength vs. temperature change in range of 30–45 °C, where the components of double ring is the same as those used in Fig. 7(b). Its temperature coefficient is obtained as $\Delta\lambda/\Delta T = 10$ pm/°C, which is similar to other fiber devices, such as FBG. It is reasonable since the main mechanism is the thermos-optic effect of silica index. Fig. 9(b) shows detailed reflection spectrum at 35 °C, the resolution of resonant peak ~ 22 MHz, much narrower than the FBG peak of ~ 10 GHz. Therefore, the detection resolution of temperature change is much enhanced. It is also easier to monitor and follow the peak variation than in the case of single ring with FBG.

4. Discussion

The advantages of double ring with FBG are demonstrated above. Further studies on lasers and sensors with the new structure of fiber ring are being undertaken. However, its susceptibility to environment conditions is not easy to avoid, similar to other fiber components. For practical applications of narrow linewidth lasers, it is necessary to pay attention on techniques of its packaging with temperature stabilization and vibration isolation.

When the double ring filter is used in narrow linewidth laser, temperature-stabilized and vibration-insulated packaging is required. Many methods used in applications of FBG filters can also be adopted here to reduce the temperature sensitivity. For example a mechanism composed of two different materials with different thermal expansion coefficient and properly designed length is used as the filter packaging in [19]. In addition, some novel materials have been developed for packaging fiber devices. It is believed the technical issues will be solved.

5. Conclusion

The fiber ring resonator with a low reflective FBG inserted has been proved an attractive slow-light element and effective for linewidth reduction of lasers. This paper proposes a new structure with a double ring to replace the single ring. It is indicated theoretically and experimentally that the narrow spacing resonances of single ring are now modulated by the Vernier effect of double ring, the spacing of envelope maxima can be greatly enlarged. By optimization of fiber lengths and split ratio of fiber couplers, mode spacing up to 5~7 FSR, SMSR up to 2.87 dB are obtained experimentally. Compared with the single ring resonator, the linewidth narrowing is measured 10 times. It is believed that such improvements will be beneficial for mode hopping suppression of narrow linewidth laser, and for enhancing the resolution of FBG sensors.

References

- [1] J. Jung and Y. W. Lee, "Continuously wavelength-tunable passband-flattened fiber comb filter based on polarization-diversified loop structure[J]," *Sci. Rep.*, vol. 7, 2017, Art. no. 8311.
- [2] A. P. Luo *et al.*, "Wavelength switchable flat-top all-fiber comb filter based on a double-loop Mach-Zehnder interferometer[J]," *Opt. Exp.*, vol. 18, no. 6, pp. 6056–6063, 2010.
- [3] C. Ciminelli *et al.*, "Label-free optical resonant sensors for biochemical applications[J]," *Progress Quantum Electron.*, vol. 37, no. 2, pp. 51–107, 2013.
- [4] W. Li *et al.*, "Mode-hopping-free single-longitudinal-mode actively Q-switched ring cavity fiber laser with an injection seeding technique[J]," *IEEE Photon. J.*, vol. 9, no. 1, Feb. 2017, Art. no. 1500607.
- [5] G. Kumar and R. Vijaya, "Dynamical bistability of a loss modulated erbium doped fiber ring laser[J]," *Appl. Phys. B*, vol. 123, no. 5, 2017, Art. no. 152.
- [6] L. Zhang *et al.*, "Multiwavelength coherent Brillouin random fiber laser with ultrahigh optical signal-to-noise ratio[J]," *IEEE J. Sel. Topics Quantum Electron.*, vol. 24, no. 3, May/June. 2018, Art. no. 0900308.
- [7] S. Fu *et al.*, "Linewidth-narrowed, linear-polarized single-frequency thulium-doped fiber laser based on stimulated Brillouin scattering effect[J]," *IEEE Photon. J.*, vol. 9, no. 4, Aug. 2017, Art. no. 1504207.
- [8] Z. Fang, K. Chin, R. R. Qu, and H. Cai, *Fundamentals of Optical Fiber Sensors*. New York, NY, USA: Wiley, 2012.
- [9] C. E. Campanella *et al.*, "Localized strain sensing with fiber Bragg-grating ring cavities," *Opt. Exp.*, vol. 21, no. 24, pp. 29435–29441, 2013.
- [10] Z. Pan, Q. Ye, H. Cai, R. Qu, and Z. Fang, "Fiber ring with long delay used as a cavity mirror for narrowing fiber laser," *IEEE Photon. Technol. Lett.*, vol. 26, no. 16, pp. 1621–1624, Aug. 2014.
- [11] Q. Ye, Z. Pan, Z. Wang, Z. Fang, H. Cai, and R. Qu. Novel, "Slow-light reflector composed of a fiber ring resonator and low-reflectivity fiber Bragg grating," *J. Lightw. Technol.*, vol. 33, no. 14, pp. 3016–3022, 2015.
- [12] Y. Okawachi *et al.*, "Tunable all-optical delays via Brillouin slow light in an optical fiber," *Phys. Rev. Lett.*, vol. 94, no. 15, 2005, Art. no. 153902.
- [13] J. T. Mok and B. J. Eggleton, "Expect more delays," *Nature*, vol. 433, pp. 811–812, 2005.
- [14] F. L. Kien, J. Q. Liang, and K. Hakuta, "Slow light produced by faroff-resonance Raman scattering," *IEEE J. Sel. Topics Quantum Electron.*, vol. 9, no. 1, pp. 93–101, Jan./Feb. 2003.
- [15] J. B. Khurgin, "Slow light in various media: A tutorial," *Adv. Opt. Photon.*, vol. 2, no. 3, pp. 287–318, 2010.
- [16] Y. Shevy, D. Shevy, R. Lee, and D. Provenzano, "Slow light laser oscillator," in *Proc. Int. Conf. Opt. Fiber Commun.*, 2010, Paper OThQ6.
- [17] J. Ctyroky, I. Richter, and M. Sinor, "Dual resonance in a waveguide-coupled ring microresonator," *Opt. Quantum Electron.*, vol. 38, no. 9–11, pp. 781–797, 2006.
- [18] H. Ishii, H. Tanobe, F. Kano, Y. Tohmori, Y. Kondo, and Y. Yoshikuni, "Quasicontinuous wavelength tuning in superstructure-grating (SSG) DBR lasers," *IEEE J. Quantum Electron.*, vol. 32, no. 3, pp. 433–441, Mar. 1996.
- [19] W. Yoffe *et al.*, "Passive temperature-compensating package for optical fiber gratings[J]," *Appl. Opt.*, vol. 34, no. 30, pp. 6859–61, 1995.
- [20] J. Gu *et al.*, "Cascaded fiber Sagnac loop-based microwave photonic multiband bandpass filter with a selectable passband frequency[J]," *Chin. Opt. Lett.*, vol. 15, no. 11, 2017, Art. no. 110603.
- [21] J. Cui *et al.*, "Stimulated Brillouin scattering evolution and suppression in an integrated stimulated thermal Rayleigh scattering-based fiber laser[J]," *Photon. Res.*, vol. 5, no. 3, pp. 233–238, 2017.
- [22] X. Dong, M. Xu, and Q. Zhang, "Optical pulse repetition rate multiplication based on series-coupled double-ring resonator[J]," *Photon. Res.*, vol. 4, no. 2, pp. 61–64, 2016.